Subcritical water extraction of *Gracilaria chorda* abbreviates lipid accumulation and obesity-induced inflammation

Laxmi Sen Thakuri[1,2], Chul Min Park[1,3], Jin Woo Park[2], Hyeon-A Kim[4] and Dong Young Rhyu[1,2,*

[1]*Department of Nutraceutical Resources, Mokpo National University, Muan 58554, Korea*
[2]*Department of Biomedicine, Health & Life Convergence Sciences, BK21 FOUR, Mokpo National University, Muan 58554, Korea*
[3]*Inhalation Toxicity Research Group, Korea Institute of Toxicology, Jeongeup 56212, Korea*
[4]*Department of Food and Nutrition, Mokpo National University, Muan 58554, Korea*

Obesity-induced inflammation is crucial in the pathogenesis of insulin resistance and type 2 diabetes. In this study, we investigated the effects of the *Gracilaria chorda* (GC) on lipid accumulation and obesity-induced inflammatory changes or glucose homeostasis in cell models (3T3-L1 adipocytes and RAW 264.7 macrophages). Samples of GC were extracted using solvents (water, methanol, and ethanol) and subcritical water (SW) at different temperatures (90, 150, and 210°C). The total phenolic content of GCSW extract at 210°C (GCSW210) showed the highest content compared to others, and GCSW210 highly inhibited lipid accumulation and significantly reduced gene expressions of peroxisome proliferator-activated receptor-γ, CCAAT/enhancer-binding protein-α, sterol regulatory element-binding protein-1c, and fatty acid synthase in 3T3-L1 adipocytes. In addition, GCSW210 effectively downregulated the pro-inflammatory cytokine regulator pathways in RAW 264.7 macrophages, including mitogen-activated protein kinase, signal transducers and activators of transcription and nuclear factor-κB. In co-culture of 3T3-L1 adipocytes and RAW 264.7 macrophages, GCSW210 significantly reduced nitric oxide production and interleukin-6 levels, and improved glucose uptake with dose-dependent manner. These findings suggest that GCSW210 improves glucose metabolism by attenuating obesity-induced inflammation in adipocytes, which may be used as a possible treatment option for managing obesity and associated metabolic disorders.

INTRODUCTION

Obesity is a metabolic condition of abnormal fat accumulation due to an energy imbalance (Spiegelman and Flier 2001). It is a significant risk factor for many serious ill-nesses such as heart disease, arthritis, and diabetes (Pi-Sunyer 1993). The critical characteristics of obesity is excessive triglycerides storage in adipose tissue, which is achieved by increase of adipocytes number and size (Hristov et al. 2019). Peroxisome proliferator-activated receptor-γ (PPAR-γ), CCAAT/enhancer-binding protein-α (C/EBP-α), sterol regulatory element-binding transcription factor 1 (SREBP1), and fatty acid synthase (FAS) are key activators of adipogenesis and lipogenesis during the differentiation of adipocytes (Sharma et al. 2017). The obese adipose tissue also forms a low-grade inflammatory environment by activating local immune cells such as macrophages (Suganami et al. 2005). Activated macrophages play an essential role in cytokine productions like interleukin-6 (IL-6) and inducible nitric oxide synthase (iNOS), thereby creating an aggravated inflammatory response between adipocytes and macrophages (Tateya et al. 2013). The obesity-associated state of chronic low-grade systemic inflammation is considered a key step in the progression of insulin resistance (IR) (Lin et al. 2020). IR is a hallmark of obesity, and is a forerunner of type 2 diabetes (Czech 2017). The previous scientific evidences indicate that factors affecting the development of IR in obesity are complex and regulated by a variety of signaling pathways.

Gracilaria chorda (GC) Holmes is a red alga belonging to the family Gracilariaceae. It is also coined as *Gracilariopsis chorda* (Taxonomy ID: 448386), which grows in Korea, Japan, China, and the western coast of the North Pacific Ocean, and is used as food and cosmetic materials (Kakita and Kamishima 2006). Previous studies have reported that *Gracilaria* sp. comprises of approximately 23.6 g 100 g^{-1} of protein, 0.7 g 100 g^{-1} of fat, and 46.9 g 100 g^{-1} of carbohydrate (Neto et al. 2018). In addition, other studies reported that GC biomass contains large amount of carbohydrate (34.4% [g g^{-1} dry weight (DW)]) and 1.5 mg 100 DW^{-1} of arachidonic acid (Meinita et al. 2013, Mohibbullah et al. 2015). Although several studies on Gracilariaceae have shown biological activities including anti-oxidant, anti-bacterial, anti-obesity, neuroprotective effect, and anti-inflammatory effects, in experimental models including cells and animals, there are few experimental studies on the biological effects of GC (Rumbaoa et al. 2009, Hiramitsu et al. 2014, Mohibbullah et al. 2015, 2016). This study aimed to investigate the effects of GC on lipid accumulation, obesity-induced inflammation, and glucose metabolism using a difference in cell cultured model of 3T3-L1 adipocytes, RAW 264.7 macrophages, and their co-culture on obesity-related factors that induce inflammation which could promote IR. Subcritical water extraction, hot water, and organic solvent extracts were prepared to analyze GC effects depending on the extracting methods.

MATERIALS AND METHODS

Reagents

Insulin, 3-(4,5-dimethylthiazol-2-yl)-2,5-diphenyl tetrazolium bromide (MTT), dimethyl sulfoxide (DMSO), dexamethasone, 3-isobutyl-1-methylxanthine (IBMX), lipopolysaccharide (LPS) from *Escherichia coli*, Oil Red O, 2-mercaptoethanol, anti–β-actin, Folin-Ciocalteu reagent, and gallic acid (GA) were purchased from Sigma Aldrich (St. Louis, MO, USA). Antibodies against PPAR-γ (sc-7273), C/EBP-α (sc-61), iNOS (sc-650), nuclear factor-κB (NF-κB; sc-372) were purchased from Santa Cruz Biotechnology (Santa Cruz, CA, USA) and c-Jun NH2-terminal kinase (JNK; #9252), p38 mitogen-activated protein kinase (p38 MAPK; #8690), and signal transducers and activators of the transcription-1 (STAT-1; #9172) were purchased from Cell Signaling Technology (Danvers, MA, USA). 2-[N-(7-nitrobenz-2-oxa-1,3-diazol-4-yl)amino]-2-deoxyglucose (2-NBDG) was purchased from Invitrogen (Carlsbad, CA, USA). Sodium carbonate, methanol, and ethanol were purchased from DUKSAN (Ansan, Korea).

Preparation of GC extracts

GC used in this study was collected from Jeollanam-do, South Korea. The taxonomic identity of seaweed was confirmed by Prof. Chan-Sun Park and the sample was preserved for reference in the herbarium of the Department of Nutraceutical Resources, Mokpo National University, South Korea. The GC extract was produced with subcritical water (SW) and several solvents (water, methanol, and ethanol) to investigate its potential. After collection, GC was washed thoroughly to remove salt. For the solvent extraction, 20 g of GC was dissolved in 200 mL of 100% EtOH; 20 g were dissolved in 100% MeOH; and 300 g were dissolved in 800 mL of water. The organic solvent extract was immersed in 100% MeOH and EtOH until the color faded, and water extract was performed at 100°C for 15

min. These extracts were filtered and evaporated under vacuum conditions and then freeze-dried for up to 72 h to yield 0.3 g of dry EtOH extract (GCE; 1.5% yield), 0.4 g of MeOH extract (GCM; 2% yield), 8 g of water extract powder (GCW; 2.67% yield). For the subcritical water extract (SWE) process, the reaction temperature for hydrolysis of raw GC was maintained at several temperatures (90, 150, and 210°C) and the extract was labeled as GCSW90, GCSW150, and GCSW210, respectively. Fresh GC (20 g) was soaked in an extraction cell with 200 mL of distilled water, and botanical extraction equipment (TPR-1, TAIATSU TECHNO, Osaka, Japan) maintained a constant pressure at 3 MPa. Then, the reaction temperature for hydrolysis was raised to 90, 150, and 210°C and the extraction was kept for 1 min. This extract was filtered and freeze-dried for up to 72 h to yield 13 g of GCSW90 (65% yield), 5.1 g of GCSW150 (25.5% yield), and 2.3 g of GCSW210 powder (11.5% yield).

Determination of the total phenolic content

The total phenolic content was determined for all each extract using the Folin-Ciocalteu method (Rumbaoa et al. 2009). Briefly, 200 μL of GC (1 mg mL^{-1}), 1.4 mL of distilled water, and 100 μL of Folin-Ciocateu reagent were mixed and allowed to stand for 30 s at 25°C. Then, 300 μL of 20% sodium carbonate solution was added to the reaction mixture and incubated at 25°C for 2 h. Finally, the absorbance of the reaction mixture was measured at 765 nm using a spectrophotometer (Immuno Mini NJ-2300; Shinshu-u, Tokyo, Japan). The standard solutions of GA (10 to100 ppm) were similarly treated to prepare the calibration curve. The results were expressed as mg gallic acid 100 g^{-1} of dry sample.

Cell culture and differentiation

3T3-L1 preadipocytes purchased from the American Type Culture Collection (ATCC; Manassas, VA, USA) were grown in Dulbecco's modified Eagle's medium (DMEM) containing 10% newborn calf serum and 1% penicillin-streptomycin. To induce differentiation, 3T3-L1 preadipocytes were cultured on a 96- or 6-well plate until confluence was reached and the culture medium was replaced with a fresh medium containing 5 μg mL^{-1} insulin, 0.5 mM IBMX, and 1 μM dexamethasone in DMEM with 10% fetal bovine serum (FBS) for 2 days. The medium was then replaced with a differentiation medium containing 5 μg mL^{-1} insulin and DMEM medium containing 10% FBS and replaced every 2 days for 8 days until cells were har-

vested (Park et al. 2013). RAW 264.7 macrophages (ATCC) were cultured in DMEM containing 10% FBS and 1% penicillin-streptomycin. Cells were maintained at 37°C with 5% CO$_2$ in a humidified incubator.

Co-culture of RAW 264.7 macrophages and 3T3-L1 adipocytes

Following the methods of Shin et al. (2016), the co-culture model was used with modification in this study. In brief, RAW 264.7 macrophages were cocultured onto differentiated 3T3-L1 adipocytes with direct contact in culture well plates. After 24 h of incubation, co-culture cells were treated with DMSO or GCSW210 extract (125 and 250 μg mL^{-1}) for a further 24 h.

Cell viability

The MTT assay was performed to evaluate the cytotoxicity of the GC extract in adipocytes and macrophages. 3T3-L1 preadipocytes were seeded into 96-well plates at a density of 1×10^4 cells per well. Differentiated adipocytes were exposed to the different concentrations of GC extracts prepared with SWE at different temperatures (90, 150, and 210°C) and different solvents (GCW, GCM, and GCE) at the concentrations of 125 to 500 μg mL^{-1} for 24 h at 37°C with 5% CO$_2$.

RAW 264.7 macrophages (1×10^4 cells per well) were seeded in 96-well plates and incubated with GCSW210 (125 or 250 μg mL^{-1}), for 24 h. The MTT solution (1 mg mL^{-1}) was added to each well. After 3 h of incubation, the MTT solution was removed and replaced by DMSO to dissolve the purple crystals. Absorbance was measured at a wavelength of 540 nm (Immuno Mini NJ-2300).

Oil Red O staining

Differentiated adipocytes were washed twice with phosphate-buffered saline (PBS) and then fixed for 30 min at 25°C with 10% formalin, prepared in PBS. Then, cells were washed twice with PBS, and stained with a filtered Oil Red O solution (0.5% in 60% isopropanol) for 1 h. Finally, cells were washed twice with distilled water, and the fat droplets in 3T3-L1 adipocytes were observed via phase-contrast microscopy.

Measurement of NO production

NO production was determined according to the previously described methods by Sharma and Rhyu (2014)

with modifications. RAW 264.7 macrophages were seeded in 96-well plates and incubated with or without 1 μg mL^{-1} LPS in the presence or absence of the GCSW210 extract. After 24 h of incubation, the supernatant was collected and incubated with Griess reagent containing a 1 : 1 mixture of 0.1% N-(1-naphthyl)-ethylene diamine dihydrochloride and 1% sulfanilamide in 5% phosphoric acid at 25°C for 5 min. Absorbance was measured at a wavelength of 540 nm (Immuno Mini NJ-2300). NO production was measured as the concentration of nitrite by comparing it to a standard curve generated using NaNO$_2$.

Western blot analysis

Cell lysates containing 20 μg of protein were separated by 10% sodium dodecyl sulfate-polyacrylamide gel electrophoresis and transferred to a nitrocellulose (NC) membrane in a western blot apparatus (Bio-Rad, Hercules, CA, USA). The NC membrane was blocked with 5% skim milk for 1 h, rinsed by Tris-buffered-saline (TBS) with Tween-20 (TBS-T buffer; 1 mol L^{-1} Tris, 5 mol L^{-1} NaCl, and 0.1% Tween-20), and incubated for overnight with anti-PPAR-γ (1 : 250), C/EBP-α (1 : 250), iNOS (1 : 500), NF-κB (1 : 1,000), JNK (1 : 1,000), p38 (1 : 1,000), and STAT (1 : 1,000) primary antibodies. The NC membrane was again washed with TBS-T buffer followed by incubation with secondary antibody (horseradish peroxidase-conjugated anti-rabbit or anti-mouse and rabbit IgG (1 : 1,000) for 1 h at 25°C. Finally, the expressed proteins were measured by analyzing the signal captured in NC using a chemiluminescent substrate and Vision-Works TMLS (Analysis Software, Upland, CA, USA).

Reverse transcription-polymerase chain reaction

RNA was isolated using TRIzol reagent (Molecular Research Center, Cincinnati, OH, USA). Reverse transcription-polymerase chain reaction (RT-PCR) was performed using Diastar 2X One-Step RT-PCR Premix (SolGent, Daejeon, Korea). RNA primers were purchased from Integrated DNA Technologies (Coralville, IA, USA) and the sequences of the oligonucleotide primers were as follows: PPAR-γ forward, 5′-ACC ACAGTTGATTTCTCCAG-3′ and reverse, 5′-TGTTGTAGAGCTGGGTCTTT-3′; FAS forward, 5′-CTGCGGAAACTTCAGGAAATG-3′ and reverse, 5′-GGTTGCTCGGAATGCTATCCAGG-3′; and sterol regulatory element-binding protein-1c (SREBP-1c) forward, 5′-CACTTCTGGAGACATCGCAAAC-3′ and reverse, 5′-TGGTAGACAACAGCCGCATC-3′. The PCR conditions were 50°C for 30 min, 95°C for 15 min and 45 cycles of

denaturation at 95°C (10 s), annealing at 60°C (10 s) and extension at 72°C (20 s). PCR products were analyzed on a Red-Safe-stained 1.5% agarose gel (iNtRON Biotechnology, Seoul, Korea). Band intensities were analyzed with UVP image acquisition and analysis software (Vision-Works, San Antonio, LX, USA).

2-NBDG uptake analysis

Fully differentiated 3T3-L1 adipocytes cocultured with RAW 264.7 macrophages for 24 h, were treated with GCSW210 for a further 24 h and followed by treatment with 2-NBDG, dissolved in PBS and incubated for 30 min. After incubation, cells were washed twice with PBS. Fluorescence was quantified using a fluorescence microplate reader (Perkin Elmer, Waltham, MA, USA) at excitation and emission wavelengths of 485 and 535 nm, respectively.

Statistical analyses

Data are expressed as the means ± standard error of the mean. All statistical analyses were performed using one-way analysis of variance and Dunnett's test using GraphPad Prism version 5.03 (GraphPad Software, Inc., San Diego, CA, USA). Significant differences were defined for $p < 0.05$.

RESULTS

Total phenolic content of GC extracts

Phenolic compounds are important plant constituents with redox properties responsible for anti-oxidant activity (Shahidi and Ambigaipalan 2015). We used Folin-Ciocalteu reagent to measure the total phenol content of each extract of GC. The results were derived from a calibration curve of GA and expressed in mg GA 100 g^{-1} dry extract weight. SWE was shown to extract phenolic compounds more effectively than the organic solvent extract. Among them, GCSW210 showed the highest phenolic content of 170 mg equivalent of GA 100 g^{-1} of the extract (Fig. 1).

Effects of GC extracts on cell cytotoxicity and lipid accumulation in 3T3-L1 adipocytes

All GC extracts did not show cytotoxicity when treated up to 500 μg mL^{-1} concentration in 3T3-L1 adipocytes (Fig. 2A). A concentration of 250 μg mL^{-1} was used to mea-
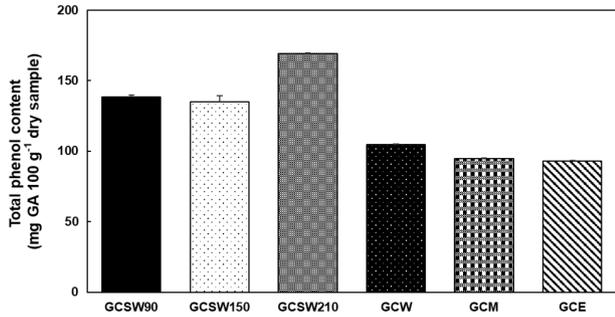
Fig. 1. Total phenolic content of *Gracilaria chorda* (GC) extracts. Phenol content was derived from a calibration curve of gallic acid (GA) and expressed in GA equivalents per 100 g dry extract weight. GCSW90, subcritical water extract of GC at 90℃; GCSW150, subcritical water extract of GC at 150℃; GCSW210, subcritical water extract of GC at 210℃; GCW, hot-water extract of GC; GCM, methanol extract of GC; GCE, ethanol extract of GC. Data are means ± standard error of the mean (n = 6).

sure the adipogenic effect of the GC extracts. GCSW210 inhibited lipid accumulation and triglyceride content most distinctly compared to other extracts (Fig. 2B & C). In addition, anti-adipogenic effects of GCSW210 were expressed in a dose-dependent manner (Fig. 3B & C). Because GCSW210 showed strong effects on lipid accumulation, further experiments were performed.

Effects of GCSW210 on the protein and mRNA expression of lipid accumulation in 3T3-L1 adipocytes

PPAR-γ and C/EBP-α are key activators of adipogenesis, and SREBP-1c control genes involved in lipid metabolism including FAS (Sharma et al. 2019). In this study,
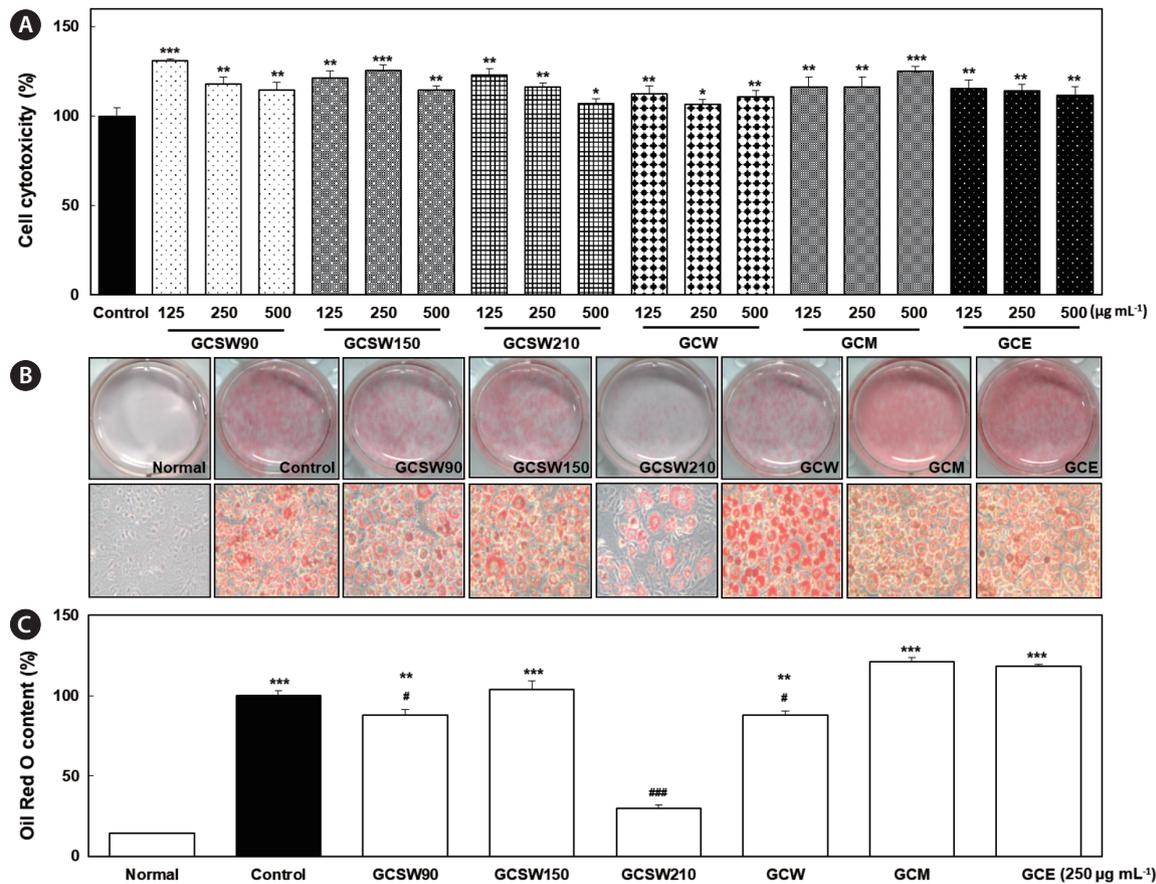

Fig. 2. Effects of *Gracilaria chorda* (GC) extracts on cell viability (A), Oil Red O stain (B), and triglyceride content (C) in 3T3-L1 adipocytes. Confluent 3T3-L1 preadipocytes were differentiated into adipocytes for 8 days (from days 0 to 8) in the presence of GC extracts. Lipid droplets were stained with Oil Red O dye. The amount of stained triglyceride content (red) was quantified at 540 nm. The concentration of the sample was 250 μg mL^{-1}. Normal, no differentiation without sample; control, differentiation without sample; GCSW90, subcritical water extract of GC at 90℃; GCSW150, subcritical water extract of GC at 150℃; GCSW210, subcritical water extract of GC at 210℃; GCW, hot-water extract of GC; GCM, methanol extract of GC; GCE, ethanol extract of GC. *$p < 0.05$, **$p < 0.01$, and ***$p < 0.001$ versus normal without differentiation; #$p < 0.05$ and ###$p < 0.001$ versus control with differentiation (one-way analysis of variance, followed by Dunnett's test). Each value represents the means ± standard error of the mean (n = 6).
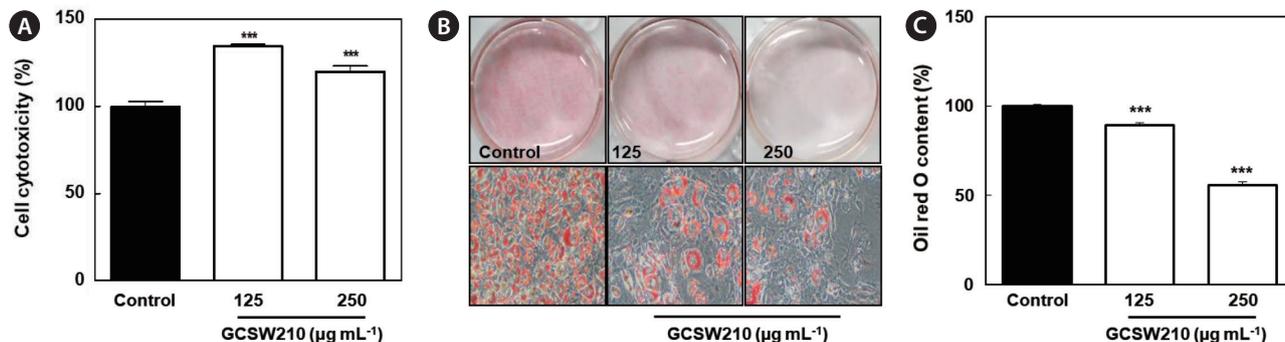
Fig. 3. Effect of GCSW210 on cell cytotoxicity (A), lipid accumulation (B), and triglyceride content (C) in 3T3-L1 adipocytes. Cells were treated with different concentrations (125 or 250 μg mL^{-1}) of GCSW210, and cell viability was measured using the MTT assay. Confluent 3T3-L1 preadipocytes were differentiated into adipocytes for 8 days (from days 0 to 8) in the presence of GCSW210. Lipid droplets were stained with Oil Red O dye. The amount of stained triglyceride (red) was quantified at 540 nm absorbance. Control, differentiation without GCSW210; GCSW210, subcritical water extract of *Gracilaria chorda* (GC) at 210℃. ***$p < 0.001$ versus control without treatment (one-way analysis of variants, followed by the Dunnett's test). Each value represents the means ± standard error of the mean (n = 6).
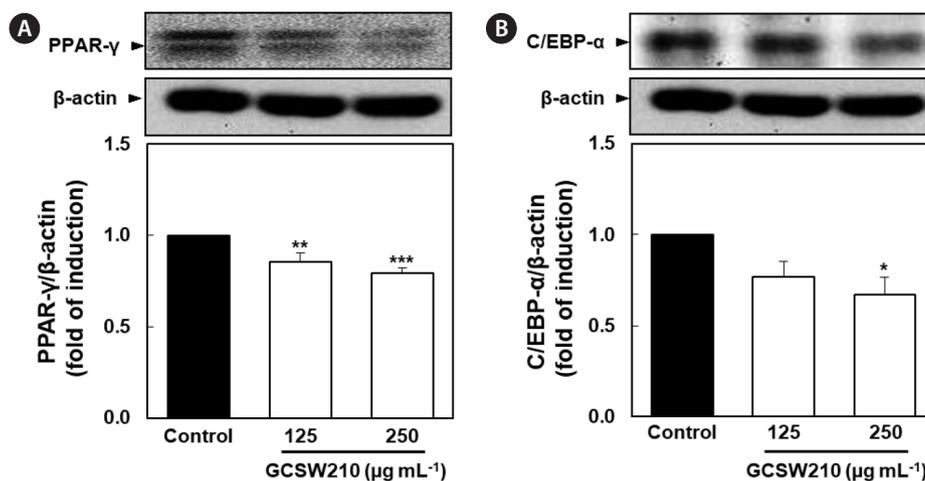

Fig. 4. Effects of GCSW210 on the protein expression of peroxisome proliferator activated receptor-γ (PPAR-γ) (A) and CCAAT/enhancer-binding protein-α (C/EBP-α) (B) in 3T3-L1 adipocytes. Control, no treatment of GCSW210; GCSW210, subcritical water extract of *Gracilaria chorda* (GC) at 210℃. *$p < 0.05$, **$p < 0.01$, and ***$p < 0.001$ versus no treatment control (one-way analysis of variants, followed by the Dunnett's test). Each value represents the means ± standard error of the mean (n = 3).

the expression of lipid regulators was found to be down-regulated in a dose-dependent manner when treated with GCSW210. Compared with the control group, the GCSW210-treated groups showed a lower expression for both regulators (Fig. 4A & B). Also, GCSW210 significantly alleviated mRNA expression of PPAR-γ, SREBP-1c, and FAS in mature 3T3-L1 adipocytes (Fig. 5).

Effects of GCSW210 on inflammation in RAW 264.7 macrophages

GCSW210 significantly inhibited the inflammatory response in LPS-treated RAW 264.7 macrophages. In Fig. 6, the induction of LPS in RAW 264.7 macrophages highly elevated NO production and nitric oxide synthase 2 (NOS2) expression, as a marker of the inflammatory response, whereas the cell viability was reduced by about 20% compared to the normal group. Treatment of GCSW210 in RAW 264.7 macrophages effectively inhibited NO production and NOS2 protein expression induced by LPS in a dose-dependent manner, enhancing cell viability.

Effects of GCSW210 on NF-κB p65, MAPK, and STAT-1 activation RAW 264.7 macrophages

The activation of NF-κB, MAPK, and STAT-1 pathways causes the transcription of inflammatory cytokines and mediators such as iNOS and tumor necrosis factor-α
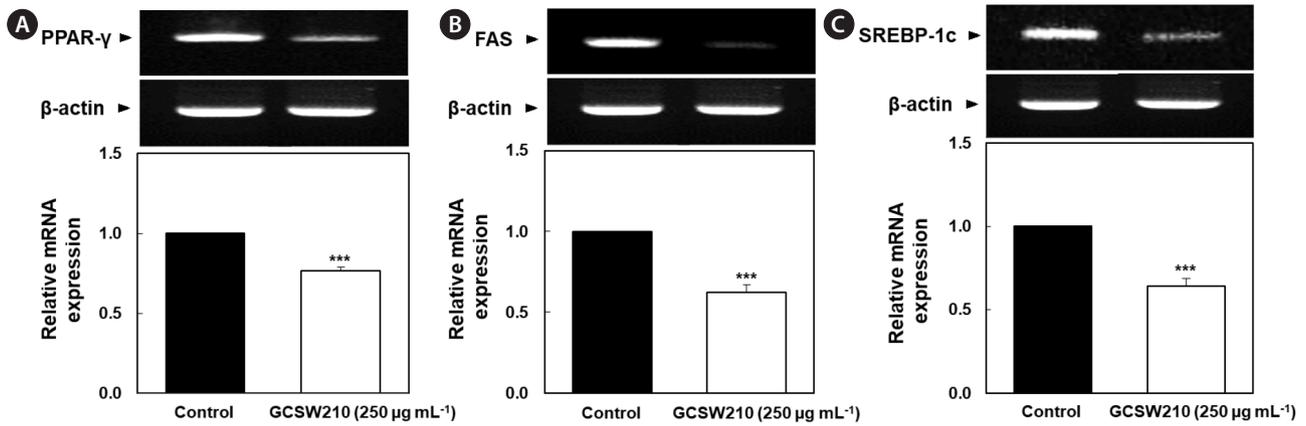
Fig. 5. Effects of GCSW210 on the mRNA expression of peroxisome proliferator activated receptor-γ (PPAR-γ) (A), fatty acid synthase (FAS) (B), and sterol regulatory element binding protein-1c (SREBP-1c) (C) in 3T3-L1 adipocytes. The concentration of GCSW210 was 250 μg mL⁻¹. Control, no treatment of GCSW210; GCSW210, subcritical water extract of *Gracilaria chorda* (GC) at 210°C. ***p < 0.001 versus no treatment control (one-way analysis of variance, followed by Dunnett's test). Each value represents the means ± standard errors of the mean (n = 3).
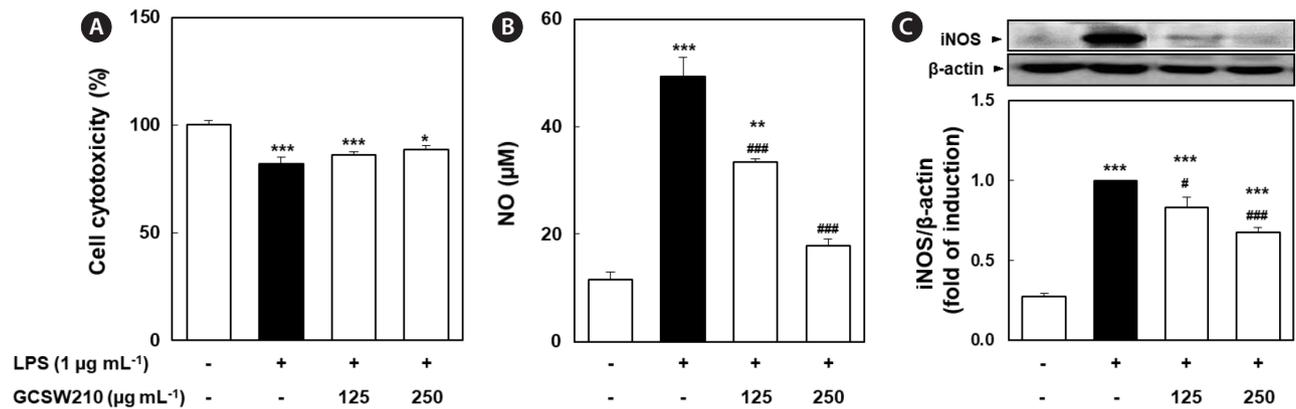

Fig. 6. Effects of GCSW210 on cell viability (A), nitric oxide (NO) production (B), and inducible nitric oxide synthase (iNOS) expression (C) in RAW 264.7 macrophages. Lipopolysaccharide (LPS) is an inducer of inflammation. GCSW210, subcritical water extract of *Gracilaria chorda* (GC) at 210°C. *p < 0.05, **p < 0.01, and ***p < 0.001 versus no treatment; #p < 0.05 and ###p < 0.001 versus LPS-induced control without GCSW210 (one-way analysis of variant, followed by the Dunnett test). Each value represents the means ± standard error of the mean (n = 6).

(TNF-α) (Bagaev et al. 2019). LPS significantly stimulated the translocation of NF-κB p65 subunit from the cytosol to the nucleus compared with no treatment in RAW 264.7 macrophages, but treatment of GCSW210 highly suppressed the translocation of NF-κB p65 in a dose-dependent manner (Fig. 7). Additionally, LPS-stimulated MAPK and STAT-1 pathways significantly inhibited by treatment of GCSW210, and there were restored almost like normal cells at the concentration of 250 μg mL⁻¹ (Fig. 8).

Effects of GCSW210 on obesity-induced inflammation and glucose metabolism in the cocultured condition of adipocytes and macrophages

A prolonged state of obesity can increase the systemic levels of pro-inflammatory cytokines, such as IL-6 (Makki et al. 2013). In co-culture of 3T3-L1 adipocytes and RAW 264.7 macrophages, GCSW210 showed no cytotoxicity up to 250 μg mL⁻¹ (Fig. 9A). The pro-inflammatory cytokine IL-6 and NO level as biomarker of inflammatory response significantly enhanced in cocultured adipocytes compared to adipocytes (Fig. 9B & C). However, the addition of GCSW210 effectively reduced IL-6 and NO production in adipocyte-macrophage co-culture system such as obesity-induced inflammation. To investigate the regulatory activity of GCSW210 on glucose metabolism in a co-culture model, glucose uptake was measured with or without insulin (Fig. 9D). In 3T3-L1 adipocytes, the treatment of insulin (100 nmol L⁻¹) or GCSW210 (250 μg mL⁻¹) significantly increased 2-NBDG uptake compared with
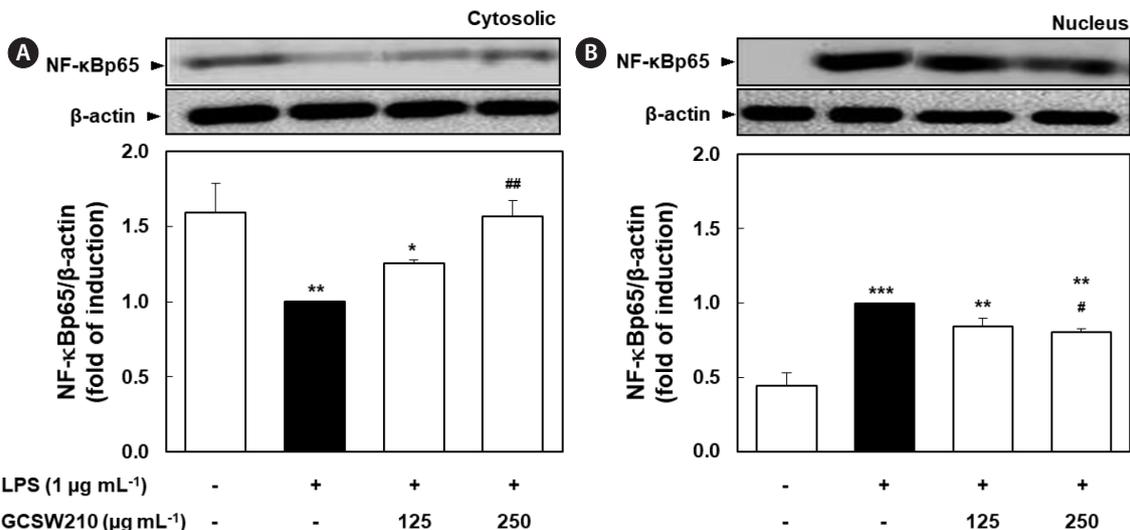
Fig. 7. Effects of GCSW210 on nuclear factor-κB (NF-κB) p65 translocation in RAW 264.7 macrophages (A & B). Lipopolysaccharide (LPS) is an inducer of inflammation. GCSW210, subcritical water extract of *Gracilaria chorda* (GC) at 210°C. *p < 0.05, **p < 0.01, and ***p < 0.001 versus no treatment; #p < 0.05 and ##p < 0.01 versus LPS-induced control without GCSW210 (one-way analysis of variant, followed by the Dunnett test). Each value represents the means ± standard error of the mean (n = 3).

Fig. 8. Effects of GCSW210 on c-Jun NH2 terminal kinase (JNK) (A), p38 (B), and signal transducers and activators of the transcription-1 (STAT-1) (C) expression in RAW 264.7 macrophages. Lipopolysaccharide (LPS) is an inducer of inflammation. GCSW210, subcritical water extract of *Gracilaria chorda* at 210°C. *p < 0.05, **p < 0.01, and ***p < 0.001 versus no treatment; #p < 0.05, ##p < 0.01, and ###p < 0.001 versus LPS-induced control without GCSW210 (one-way analysis of variant, followed by the Dunnett test). Each value represents the means ± standard error of the mean (n = 3).
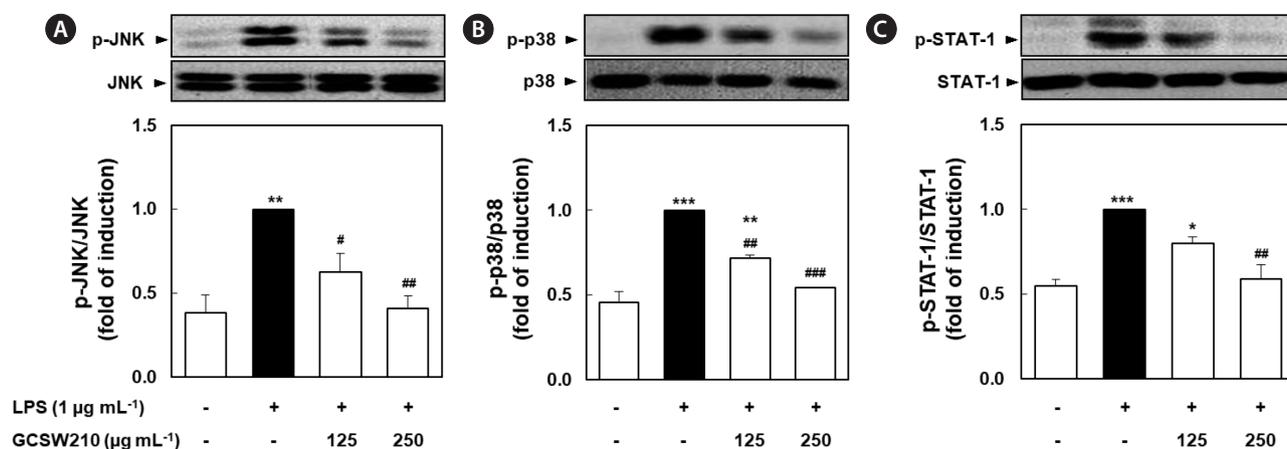
no treatment. However, 2-NBDG uptake significantly decreased in obesity-induced inflammation condition of adipocyte-macrophage co-culture compared with adipocytes, suggesting the induction of IR. Nevertheless, the reduced 2-NBDG uptake in obesity-related IR condition of co-culture system was almost restored to normal by treatment of insulin or GCSW210, respectively. In addition, when insulin and GCSW210 were treated together in adipocyte-macrophage co-culture system, 2-NBDG uptake was higher than that of the single treatment. This

indicates that GCSW210 could improve glucose metabolism by regulating obesity-stimulated inflammation and IR in adipocyte-macrophage co-culture system.

DISCUSSION

In this study, GC was extracted using subcritical water or organic solvents, and GCSW210 contained the highest phenolic content. These results showed that GCSW210
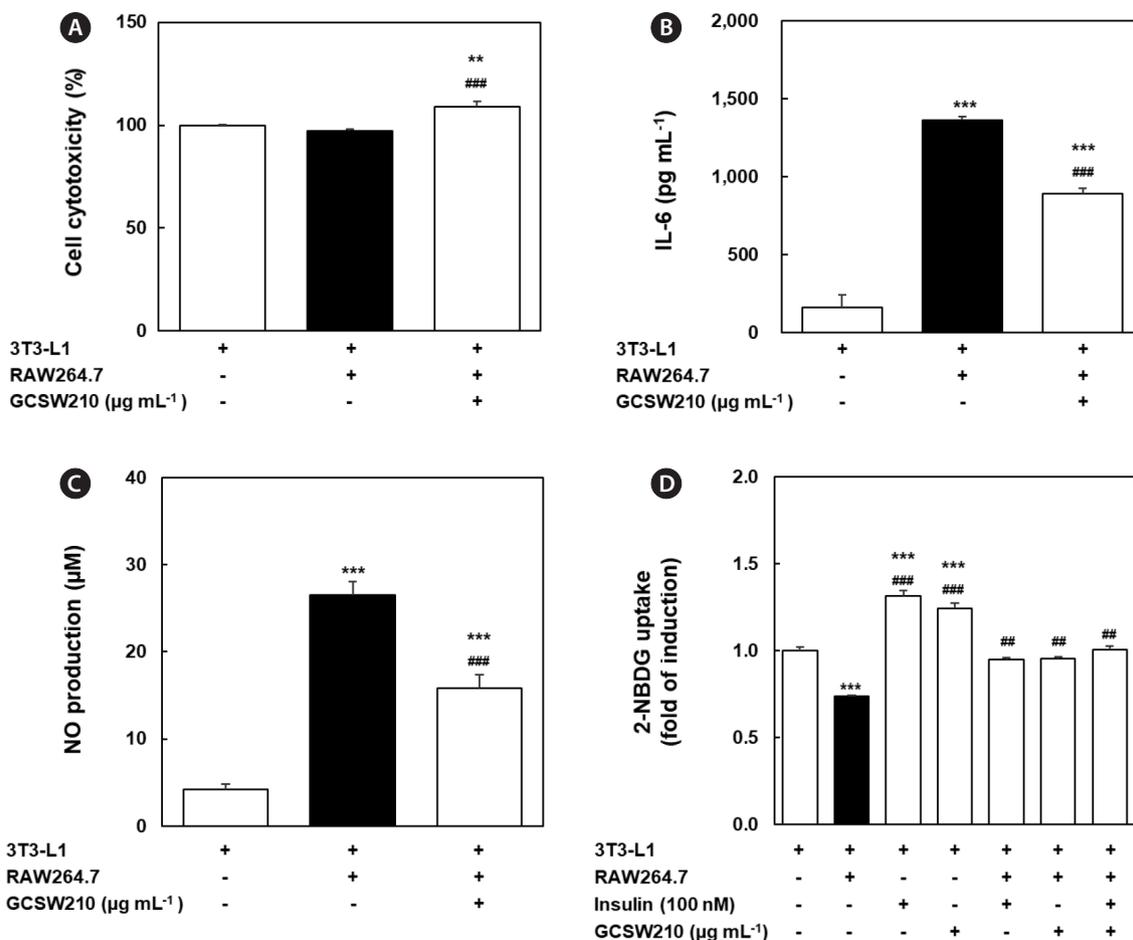
Fig. 9. Effects of GCSW210 on cytotoxicity (A), interleukin-6 (IL-6) level (B), nitric oxide (NO) production (C), and glucose uptake (D) in the co-culture of 3T3-L1 adipocytes and RAW 264.7 macrophages. 3T3-L1 adipocytes were cocultured with RAW 264.7 macrophages for 24 h, followed by treatment with GCSW210 at 250 µg mL^{-1} for a further 24 h. Glucose uptake was measured using 2-[N-(7-nitrobenz-2-oxa-1,3-diazol-4-yl)amino]-2-deoxyglucose (2-NBDG) in the presence or absence of 100 nM insulin. GCSW210, subcritical water extract of *Gracilaria chorda* at 210°C. **p < 0.01 and ***p < 0.001 versus control; ##p < 0.01 and ###p < 0.001 versus adipocyte-macrophage co-culture condition (one-way analysis of variant, followed by the Dunnett test). Each value represents the means ± standard error of the mean (n = 6).

strongly inhibits lipid accumulation in 3T3-L1 adipocytes and reduces the gene expression of major adipogenic and lipogenic regulators during differentiation or lipid accumulation. Moreover, the activation of NO production and inflammation-related genes, including iNOS, JNK, p38, STAT-1, and NF-κB, effectively regulated by GCSW210 treatment in RAW 264.7 macrophages. Finally, GCSW210 has been proven to improve glucose metabolism via controlling obesity-induced inflammatory responses in the co-culture system of adipocytes-macrophages.

Recently, SWE has become a popular alternative technology because it is a novel green technique for extracting non-polar compounds from natural resources using only water for a short time (Coura et al. 2015). Also, SWE is replacing conventional organic solvents because it is cheap, safe, and efficient. In addition, it provides high biological activities of extracts while precluding any toxic solvents (Kumar et al. 2011). Kapalavavi et al. (2021) reported that SWE of *Salvia militiorrhiza* is more efficient in extracting anticancer agents than traditional herb decoction (Kapalavavi et al. 2021). In this study, GC subcritical water extract was prepared at different temperatures and compared with organic solvent extracts such as hot water, methanol, and ethanol. GCSW210 showed the highest phenolic content with the lowest cytotoxicity and strongest inhibition of lipid accumulation on adipocytes. Therefore, GCSW210 is not only more effective in extracting phenolic compounds from GC but also strongly inhibits lipid accumulation in 3T3-L1 adipocytes.

Adipose tissue plays important roles in regulating lipid

and glucose homeostasis. Obesity is characterized by excessive fat accumulation in adipose tissue, which is composed of adipocytes. Therefore, an increase in the number and size of differentiated mature adipocytes is closely related to the development of obesity. Adipogenesis or lipogenesis is regulated by a number of transcription factors such as PPAR-γ, C/EBP-α, and SREBP-1c (Chang and Kim 2019). Several reports have shown that downregulation of PPAR-γ, C/EBP-α, and SREBP-1c expression have successfully prevented adipocyte maturation and lipid accumulations in 3T3-L1 cells (Ono and Fujimori 2011, Inafuku et al. 2013, Park et al. 2019). As expected, the expression of major adipogenic or lipogenic factors naturally increased in the untreated group, whereas the GCSW210-treated group showed a significant reduction of transcription factors promoting adipogenesis or lipogenesis. Furthermore, GCSW210 significantly reduced expression of the fat-forming enzyme such as FAS. These results explain that GCSW210 contains properties that could restrict intracellular fat accumulation by regulating the expression of master adipogenesis or lipogenesis.

Excessive lipid accumulation, one of the significant factors in developing obesity (van Herpen and Schrauwen-Hinderling 2008), can escalate pro-inflammatory cytokines associated with an increased number of macrophages in adipose tissue (Sharma et al. 2019). Macrophages and adipocytes interact promotes low systemic inflammation response in adipose tissue, leading to the activation of transcription factor NF-κB in macrophages and pro-inflammatory cytokines production (Martos-Rus et al. 2021). NF-κB translocation in inflammatory conditions activates the p38-MAPK pathway, leading to a prolonged inflammation where STAT-1 plays an important role in the cytokine productions (Sun et al. 2017, Bagaev et al. 2019). The NF-κB and MAPK pathways are common inflammatory signaling pathways whose activation causes pro-inflammatory cytokines, including IL-6, IL-8, and TNF-α (Park et al. 2015, Lee et al. 2022). In this study, LPS-treated RAW 264.7 cells showed an increased NO production and iNOS2 and NF-κB expression, indicating an inflammatory response. Furthermore, the protein expression of MAPK (JNK and p38) and STAT-1 were significantly elevated in the LPS-treated group compared with normal group. In contrast, the GCSW210 group effectively recovered similarly to the normal group, displaying the anti-inflammatory effects by reducing cytokine production. Our data suggest that anti-inflammatory effect of GCSW210 can be regulated the chronic inflammatory condition that occurs in obesity.

The dysregulation of obesity-induced adipokines increases lipolysis, causing an increase in levels of free fatty acids which impairs lipid metabolism and triggers IR (Kim et al. 2015). Several studies have demonstrated that obesity is associated with an increased risk of developing IR (Rotter et al. 2003, Vandanmagsar et al. 2011, Panee 2012, Nandipati et al. 2017). Also, the imbalance of glucose homeostasis is the key feature of several metabolic disorder diseases (Rosen and Spiegelman 2006, Park et al. 2014). When the adipocytes were cocultured with macrophages, glucose uptake was significantly decreased with increased IL-6 levels and NO productions compared with that in culture without macrophages, suggesting that IR is induced due to the increased cytokine productions in the co-culture of adipocytes and macrophages. GCSW210 treatment significantly improved glucose uptake, and cotreatment with GCSW210 and insulin further enhanced glucose uptake in the co-culture of adipocytes and macrophages, revealing that GCSW210 escalates the glucose uptake mechanism. These results indicate that GCSW210 contributed to an increase of glucose uptake rate by inhibiting adipokines and inflammation response in obesity condition.

This study provides an initial step in exploring the anti-obesity and anti-diabetic activities of GCSW210. Its mechanism is associated with the control of lipid metabolism, including adipogenesis and lipogenesis. Also, the prevention of obesity-induced inflammation state with increased glucose uptake was found in cocultured 3T3-L1 adipocytes and RAW 264.7 macrophages. However, further studies are required to explore the role of GCSW210 in the insulin sensitivity pathway in obese and insulin resistance-induced models.

Taken together, GCSW210 showed the potential to regulate the obese-induced inflammation response involved in the desensitization of insulin action, giving a new approach for the management of obesity and metabolic disorders. Further studies regarding the effect of GCSW210 are required to understand the mechanism of actions triggered to maintain the stability in obesity-induced inflammation and glucose homeostasis including the insulin signaling mechanism, and to identify the possible active compounds responsible for the anti-obesity and anti-diabetic properties of GCSW210, providing an opportunity to develop a new class of drugs.

CONFLICTS OF INTEREST

The authors declare that they have no potential conflicts of interest.

REFERENCES

Bagaev, A. V., Garaeva, A. Y., Lebedeva, E. S., Pichugin, A. V., Ataullakhanov, R. I. & Ataullakhanov, F. I. 2019. Elevated pre-activation basal level of nuclear NF-κB in native macrophages accelerates LPS-induced translocation of cytosolic NF-κB into the cell nucleus. Sci. Rep. 9:4563.

Chang, E. & Kim, C. Y. 2019. Natural products and obesity: a focus on the regulation of mitotic clonal expansion during adipogenesis. Molecules 24:1157.

Coura, C. O., Souza, R. B., Rodrigues, J. A. G., Vanderlei, E, de. S. O., de Araújo, I. W. F., Ribeiro, N. A., Frota, A. F., Ribeiro, K. A., Chaves, H. V., Pereira, K. M. A., da Cunha, R. M. S., Bezerra, M. M. & Benevides, N. M. B. 2015. Mechanisms involved in the anti-inflammatory action of a polysulfated fraction from *Gracilaria cornea* in rats. PLoS ONE 10:e0119319.

Czech, M. P. 2017. Insulin action and resistance in obesity and type 2 diabetes. Nat. Med. 23:804–814.

Hiramitsu, M., Shimada, Y., Kuroyanagi, J., Inoue, T., Katagiri, T., Zang, L., Nishimura, Y., Nishimura, N. & Tanaka, T. 2014. Eriocitrin ameliorates diet-induced hepatic steatosis with activation of mitochondrial biogenesis. Sci. Rep. 4:3708.

Hristov, I., Mocanu, V., Zugun-Eloae, F., Labusca, L., Cretu-Silivestru, I., Oboroceanu, T., Tiron, C., Tiron, A., Burlacu, A., Pinzariu, A. C., Armasu, I., Neagoe, R. M., Covic, A., Scripcariu, V. & Timofte, D. V. 2019. Association of intracellular lipid accumulation in subcutaneous adipocyte precursors and plasma adipokines in bariatric surgery candidates. Lipids Health Dis. 18:141.

Inafuku, M., Nugara, R. N., Kamiyama, Y., Futenma, I., Inafuku, A. & Oku, H. 2013. *Cirsium brevicaule* A. GRAY leaf inhibits adipogenesis in 3T3-L1 cells and C57BL/6 mice.

Lipids Health Dis. 12:124.

Kakita, H. & Kamishima, H. 2006. Effects of environmental factors and metal ions on growth of the red alga *Gracilaria Chorda* Holmes (Gracilariales, Rhodophyta). J. Appl. Phycol. 18:469–474.

Kapalavavi, B., Doctor, N., Zhang, B. & Yang, Y. 2021. Subcritical water extraction of *Salvia miltiorrhiza*. Molecules 26:1634.

Kim, C. -S., Kwon, Y., Choe, S. -Y., Hong, S. -M., Yoo, H., Goto, T., Kawada, T., Choi, H. -S., Joe, Y., Chung, H. T. & Yu, R. 2015. Quercetin reduces obesity-induced hepatosteatosis by enhancing mitochondrial oxidative metabolism via heme oxygenase-1. Nutr. Metab. 12:33.

Kumar, M. S. Y., Dutta, R., Prasad, D. & Misra, K. 2011. Subcritical water extraction of antioxidant compounds from Seabuckthorn (*Hippophae rhamnoides*) leaves for the comparative evaluation of antioxidant activity. Food Chem. 127:1309–1316.

Lee, H. G., Nagahawatta, D. P., Liyanage, N. M., Jayawardhana, H. H. A. C. K., Yang, F., Je, J. G., Kang, M. C., Kim, H. S., Jeon, Y. J., Lee, H. G. & Nagahawatta, D. P. 2022. Structural characterization and anti-inflammatory activity of fucoidan isolated from *Ecklonia maxima* stipe. Algae 37:239–247.

Lin, T. -Y., Chiu, C. -J., Kuan, C. -H., Chen, F. -H., Shen, Y. -C., Wu, C. -H. & Hsu, Y. -H. 2020. IL-29 promoted obesity-induced inflammation and insulin resistance. Cell. Mol. Immunol. 17:369–379.

Makki, K., Froguel, P. & Wolowczuk, I. 2013. Adipose tissue in obesity-related inflammation and insulin resistance: cells, cytokines, and chemokines. ISRN Inflamm. 2013:139239.

Martos-Rus, C., Katz-Greenberg, G., Lin, Z., Serrano, E., Whitaker-Menezes, D., Domingo-Vidal, M., Roche, M., Ramaswamy, K., Hooper, D. C., Falkner, B. & Martinez Cantarin, M. P. 2021. Macrophage and adipocyte interaction as a source of inflammation in kidney disease. Sci. Rep. 11:2974.

Meinita, M. D. N., Marhaeni, B., Winanto, T., Jeong, G. T., Khan, M. N. A. & Hong, Y. -K. 2013. Comparison of agarophytes (*Gelidium*, *Gracilaria*, and *Gracilariopsis*) as potential resources for bioethanol production. J. Appl. Phycol. 25:1957–1961.

Mohibbullah, M., Hannan, M. A., Choi, J. -Y., Bhuiyan, M. M. H., Hong, Y. -K., Choi, J. S., Choi, I. S. & Moon, I. S. 2015. The edible marine alga *Gracilariopsis chorda* alleviates hypoxia/reoxygenation-induced oxidative stress in cultured hippocampal neurons. J. Med. Food 18:960–971.

Mohibbullah, M., Hannan, M. A., Park, I.-S., Moon, I. S. & Hong, Y.-K. 2016. The edible red seaweed *Gracilariopsis*

chorda promotes axodendritic architectural complexity in hippocampal neurons. J. Med. Food 19:638–644.

Nandipati, K. C., Subramanian, S. & Agrawal, D. K. 2017. Protein kinases: mechanisms and downstream targets in inflammation-mediated obesity and insulin resistance. Mol. Cell. Biochem. 426:27–45.

Neto, R. T., Marçal, C., Queirós, A. S., Abreu, H., Silva, A. M. S. & Cardoso, S. M. 2018. Screening of *Ulva rigida*, *Gracilaria* sp., *Fucus vesiculosus* and *Saccharina latissima* as functional ingredients. Int. J. Mol. Sci. 19:2987.

Ono, M. & Fujimori, K. 2011. Antiadipogenic effect of dietary apigenin through activation of AMPK in 3T3-L1 cells. J. Agric. Food Chem. 59:13346–13352.

Panee, J. 2012. Monocyte chemoattractant protein 1 (MCP-1) in obesity and diabetes. Cytokine 60:1–12.

Park, C. H., Rhyu, D. Y., Sharma, B. R. & Yokozawa, T. 2013. Inhibition of preadipocyte differentiation and lipid accumulation by 7-*O*-galloyl-d-sedoheptulose treatment in 3T3-L1 adipocytes. Biomed. Prev. Nutr. 3:319–324.

Park, J., Min, J. -S., Kim, B., Chae, U. -B., Yun, J. W., Choi, M. S., Kong, I. -K., Chang, K. -T. & Lee, D. -S. 2015. Mitochondrial ROS govern the LPS-induced pro-inflammatory response in microglia cells by regulating MAPK and NF-κB pathways. Neurosci. Lett. 584:191–196.

Park, J., Um, J. I., Jo, A., Lee, J., Jung, D. -W., Williams, D. R. & Park, S. B. 2014. Impact of molecular charge on GLUT-specific cellular uptake of glucose bioprobes and in vivo application of the glucose bioprobe, GB2-Cy3. Chem. Commun. 50:9251–9254.

Park, Y. -J., Seo, D. -W., Ju, J. -Y., Cha, Y. -Y. & An, H. -J. 2019. The antiobesity effects of Buginawa in 3T3-L1 preadipocytes and in a mouse model of high-fat diet-induced obesity. BioMed Res. Int. 2019:3101987.

Pi-Sunyer, F. X. 1993. Medical hazards of obesity. Ann. Intern. Med. 119:655–660.

Rosen, E. D. & Spiegelman, B. M. 2006. Adipocytes as regulators of energy balance and glucose homeostasis. Nature 444:847–853.

Rotter, V., Nagaev, I. & Smith, U. 2003. Interleukin-6 (IL-6) induces insulin resistance in 3T3-L1 adipocytes and is, like IL-8 and tumor necrosis factor-alpha, overexpressed in human fat cells from insulin-resistant subjects. J. Biol. Chem. 278:45777–45784.

Rumbaoa, R. G. O., Cornago, D. F. & Geronimo, I. M. 2009. Phenolic content and antioxidant capacity of Philippine sweet potato (*Ipomoea batatas*) varieties. Food Chem. 113:1133–1138.

Shahidi, F. & Ambigaipalan, P. 2015. Phenolics and polyphenolics in foods, beverages and spices: antioxidant activity and health effects – A review. J. Funct. Foods 18:820–897.

Sharma, B. R., Kim, H. J., Kim, M. S., Park, C. M. & Rhyu, D. Y. 2017. *Caulerpa okamurae* extract inhibits adipogenesis in 3T3-L1 adipocytes and prevents high-fat diet–induced obesity in C57BL/6 mice. Nutr. Res. 47:44–52.

Sharma, B. R. & Rhyu, D. Y. 2014. Anti-diabetic effects of *Caulerpa lentillifera*: stimulation of insulin secretion in pancreatic β-cells and enhancement of glucose uptake in adipocytes. Asian Pac. J. Trop. Biomed. 4:575–580.

Sharma, K., Adhikari, D., Kim, H. J., Oh, S. -H., Oak, M. -H. & Yi, E. 2019. *Citrus junos* fruit extract facilitates anti-adipogenic activity of *Garcinia cambogia* extract in 3T3-L1 adipocytes by reducing oxidative stress. J. Nanosci. Nanotechnol. 19:915–921.

Shin, H. -S., Kang, S. -I., Park, D. -B. & Kim, S. J. 2016. Resveratrol suppresses inflammatory responses and improves glucose uptake in adipocytes interacted with macrophages. Genes Genomics 38:137–143.

Spiegelman, B. M. & Flier, J. S. 2001. Obesity and the regulation of energy balance. Cell 104:531–543.

Suganami, T., Nishida, J. & Ogawa, Y. 2005. A paracrine loop between adipocytes and macrophages aggravates inflammatory changes: role of free fatty acid and tumor necrosis factor alpha. Arterioscler. Thromb. Vasc. Biol. 25:2062–2068.

Sun, Y., Zhang, D., Mao, M., Lu, Y. & Jiao, N. 2017. Roles of p38 and JNK protein kinase pathways activated by compound cantharidin capsules containing serum on proliferation inhibition and apoptosis of human gastric cancer cell line. Exp. Ther. Med. 14:1809–1817.

Tateya, S., Kim, F. & Tamori, Y. 2013. Recent advances in obesity-induced inflammation and insulin resistance. Front. Endocrinol. 4:93.

Vandanmagsar, B., Youm, Y. -H., Ravussin, A., Galgani, J. E., Stadler, K., Mynatt, R. L., Ravussin, E., Stephens, J. M. & Dixit, V. D. 2011. The NLRP3 inflammasome instigates obesity-induced inflammation and insulin resistance. Nat. Med. 17:179–188.

van Herpen, N. A. & Schrauwen-Hinderling, V. B. 2008. Lipid accumulation in non-adipose tissue and lipotoxicity. Physiol. Behav. 94:231–241.